HHS Public Access

Author manuscript

Sci Signal. Author manuscript; available in PMC 2022 August 22.

Published in final edited form as:

Sci Signal. ; 13(644): . doi:10.1126/scisignal.aau2803.

Oxidative crosslinking of fibronectin confers protease resistance and inhibits cellular migration

Morgan L. Locy[1], **Sunad Rangarajan**[1], **Sufen Yang**[1], **Mark R. Johnson**[1], **Karen Bernard**[1], **Ashish Kurundkar**[1], **Nathaniel B. Bone**[1], **Jaroslaw W. Zmijewski**[1], **Jaeman Byun**[2], **Subramaniam Pennathur**[2,3], **Yong Zhou**[1], **Victor J. Thannickal**[1,*]

[1]Division of Pulmonary, Allergy, and Critical Care Medicine, Department of Medicine, University of Alabama, Birmingham, AL 35294

[2]Division of Nephrology, Department of Internal Medicine, University of Michigan, Ann Arbor, MI 48109

[3]Computational Medicine and Biology, University of Michigan, Ann Arbor, MI 48109

Abstract

The oxidation of tyrosine residues to generate *o,o'*-dityrosine crosslinks in extracellular proteins is necessary for the proper function of the extracellular matrix (ECM) in various contexts in invertebrates. Tyrosine oxidation is also required for the biosynthesis of thyroid hormone in vertebrates, and there is evidence for oxidative crosslinking reactions occurring in extracellular proteins secreted by myofibroblasts. The ECM protein fibronectin circulates in the blood as a globular protein that dimerizes through disulfide bridges generated by cysteine oxidation. We found that cellular (fibrillar) fibronectin on the surface of transforming growth factor-β1 (TGF-β1)–activated human myofibroblasts underwent multimerization by *o,o'*-dityrosine crosslinking under reducing conditions that disrupt disulfide bridges, but soluble fibronectin did not. This reaction on tyrosine residues required both the TGF-β1–driven production of hydrogen peroxide and the presence of myeloperoxidase (MPO) derived from inflammatory cells, which are active participants in wound healing and fibrogenic processes. Oxidative crosslinking of matrix fibronectin attenuated both epithelial and fibroblast migration and conferred resistance to proteolysis by multiple proteases. The abundance of circulating *o,o'*-dityrosine–modified fibronectin was increased in a murine model of lung fibrosis and in human subjects with interstitial lung disease (ILD) compared to control healthy subjects. These studies indicate that tyrosine can undergo stable, covalent linkages in fibrillar fibronectin under inflammatory conditions and that this modification affects the migratory behavior of cells on such modified matrices, suggesting that this modification may play a role in both physiologic and pathophysiologic tissue repair.

*Corresponding Author. vthannickal@uabmc.edu.

Author contributions: MLL designed the project, performed experiments, interpreted the data, and wrote the manuscript; SR, KB, AK, NBB, JWZ, and YZ contributed to experimental planning and analysis; SY and MRJ contributed to performing experiments and analysis; JB and SP contributed to MS analyses; VJT designed the project, interpreted the data, and wrote the manuscript.

Competing interests: The authors declare that they have no competing interests.

INTRODUCTION

Protein oxidation occurs in normal physiological processes as a mechanism of signal transduction and in pathological states as a result of oxidative stress (1). Oxidation of cysteine, the most widely studied amino acid to undergo oxidation, leads to variable oxidation states of its thiol side chain that may result in disulfide bond formation to facilitate protein folding in the endoplasmic reticulum (2). Other amino acids, such as methionine and tryptophan, also undergo oxidative modifications, although the physiologic and pathologic implications of these modifications are less well defined (3).

In invertebrate species, tyrosine oxidation can result in the formation of dityrosine crosslinks on substrate proteins with varied physiologic functions (4–7). In each of these contexts, dityrosine crosslinking depends on the enzymatic generation of hydrogen peroxide (H_2O_2) that oxidizes the iron of heme peroxidases (hPx). The oxidized heme iron catalyzes a one-electron reduction at the ortho position of the phenol side chain of tyrosine to generate tyrosyl radicals that combine to form a stable, covalent bond (*o,o'*-dityrosine). Upon fertilization, the extracellular envelope of sea urchin eggs rapidly undergoes *o,o'*-dityrosine crosslinking by ovoperoxidase to protect against polyspermia, microbes, and mechanical stress (8). *Caenorhabditis elegans* dual oxidase (Duox), an enzyme that contains functional hPx and nicotinamide adenine dinucleotide phosphate (NADPH) oxidase domains, catalyzes *o,o'*-dityrosine protein crosslinking that stabilizes the cuticular extracellular matrix (7). In *Drosophila melanogaster*, *o,o'*-dityrosine protein crosslinking catalyzed by a homologous dual oxidase stabilizes the extracellular cuticle of the wings (4).

Although tyrosine oxidation by thyroid peroxidase, a member of the hPx family, is essential for the synthesis of thyroid hormone, normal physiologic functions for *o,o'*-dityrosine crosslinking for normal physiologic function in vertebrates have not been identified. We have previously observed that proteins in the extracellular space around myofibroblasts undergo oxidative crosslinking reactions in the presence of a hPx, suggesting *o,o'*-dityrosine formation (9), although neither the modified protein(s) nor functional consequences of these modifications were identified. In this study, we sought to determine whether extracellular matrix (ECM) proteins are susceptible to *o,o'*-dityrosine crosslinking and, if so, identify the physiologic or pathophysiologic consequences of this protein oxidation.

Here, we identified fibronectin as a preferred target of *o,o'*-dityrosine crosslinking in the ECM; this reaction required hPx activity, such as that contributed by myeloperoxidase (MPO) from inflammatory cells, and a source of H_2O_2 generated by a member of the NADPH oxidase (NOX) family of oxidoreductases, such as that induced by the pro-fibrotic cytokine, transforming growth factor-β1 (TGF-β1). *o,o'*-dityrosine crosslinking of fibronectin made it resistant to protease degradation and altered its structural or signaling properties to retard cellular migration. Oxidized moieties of fibronectin with *o,o'*-dityrosine modifications were increased in the plasma of mice subjected to experimental lung fibrosis and in human subjects with fibrotic interstitial lung disease (ILD).

RESULTS

Fibronectin is a tyrosine-rich ECM protein

The ECM undergoes rapid and dynamic changes in response to tissue injury, inflammation, and repair (10). Posttranslational modifications that mediate ECM protein crosslinking through lysine and glutamine residues, catalyzed by lysyl oxidase and transglutaminase, respectively, have been described (11, 12). We previously reported that hPxs mediate crosslinking reactions, suggestive of *o,o'*-dityrosine formation within the extracellular space of human lung fibroblasts stimulated with TGF-1 (9). Based on the premise that this chemical reaction is likely to depend on both the number of available tyrosine residues as well as the accessibility of specific tyrosine residues to the active sites of hPxs, we surveyed the number of tyrosine residues that are present in several candidate ECM proteins to identify which may be particularly susceptible to *o,o'*-dityrosine crosslinking. We observed that fibronectin, a key protein in tissue injury and repair processes, contained the highest density of tyrosine residues (100 tyrosines out of 2386 total amino acids in fibronectin, or 4.2% tyrosine; Uniprot #PO2751) (Table 1). These data motivated us to explore whether fibronectin–associated tyrosines within the ECM may be a target of hPx-mediated *o,o'*-dityrosine crosslinking.

Tyrosine residues in cellular fibronectin are susceptible to MPO-mediated o,o'*-dityrosine crosslinking*

To determine whether fibronectin was susceptible to *o,o'*-dityrosine crosslinking, we employed a cell culture model of human lung fibroblasts stimulated with TGF-1, which increases the production extracellular H_2O_2 (13). Fibroblasts activated to generate H_2O_2 were incubated with either of two exogenous hPxs – MPO, a mammalian hPx that is abundantly produced at sites of tissue inflammation by neutrophils and macrophages (14, 15), or horseradish peroxidase (HRP) – for defined time periods prior to cell lysis (Fig. 1A). Western blot analysis of extracts from these cells under reducing conditions demonstrated higher than expected molecular weight (MW) species under conditions of endogenous H_2O_2 production and the presence of the hPxs, MPO and HRP (Fig. 1B). HRP, a plant-derived hPx that catalyzes *o,o'*-dityrosine formation, appeared to more efficiently catalyze the formation of this higher MW species of fibronectin in comparison to MPO, which is consistent with more promiscuous activity of HRP (16). To determine the potential effects of endogenous, cell-derived MPO, we incubated activated myofibroblasts with polymorphonuclear leukocytes (PMNs) isolated from wild-type ($Mpo^{+/+}$) and MPO-deficient ($Mpo^{-/-}$) mice. Similar to that observed with exogenous hPxs, the higher MW species of fibronectin were detected in the presence of PMNs from $Mpo^{+/+}$ mice (Fig. 1C). The occurrence of the high MW species at around 540 kDa suggested the potential formation of fibronectin homodimers (Fig. 1D).

To define the relative specificity of *o,o'*-dityrosine crosslinking for fibronectin, we used a tyrosine analog conjugated to biotin, biotin-tyramide (Fig. 1, E and F), as bait to assess whether this reaction occurred more prominently with fibronectin than with other ECM proteins. Using the same cell culture model of TGF-1–stimulated human lung fibroblasts (Fig. 1A), we added biotin-tyramide with MPO and probed the biotinylated proteins with

streptavidin to identify proteins that crosslink with biotinylated tyramide. We identified two major bands, one at ~270 and another at 125–140 kDa (Fig. 1G). Based on our prior observations of fibronectin crosslinking (Fig. 1, B and C), the finding of biotin-tyramide reacting with a protein of ~270 kDa, and the responsiveness of this crosslinking to TGF-1 stimulation, we suspected that this band likely corresponded to fibronectin. To confirm that biotin-tyramide crosslinking targeted fibronectin, we performed neutravidin pulldown of extracts from the experiments with biotin-tyramide and probed for fibronectin; the results clearly demonstrated that under conditions when *o,o'*-dityrosine crosslinking is expected to occur, including even in low concentrations of H_2O_2 in the absence of the TGF-β1, we detected fibronectin reactivity that was markedly increased by the addition of MPO (Fig. 1, H to J). Together, these studies provide evidence that endogenous fibronectin, in the presence of extracellular H_2O_2 and MPO, could undergo posttranslational modifications involving *o,o'*-dityrosine crosslinking.

To further characterize fibronectin *o,o'*-dityrosine crosslinking in situ, we performed immunofluorescence studies with tyramide-conjugated cyanine 5 (tyramide-Cy5) and fibronectin (Fig. 2). Using the established protocol to induce ECM crosslinking by TGF-β1 and MPO (Fig. 1A), we detected increased pericellular tyramide-Cy5 fluorescence in cells treated with both TGF-1 and MPO (Fig. 2A). This tyramide-Cy5 fluorescence decreased when cells were pretreated with an inhibitor of hPxs and MPO (sodium azide), catalase (which competes with hPx to reduce H_2O_2), a flavoenzyme inhibitor that blocks TGF-β1–induced H_2O_2 (DPI, diphenylene iodonium), or L-tyrosine (which competes with the reaction of endogenous fibronectin-associated tyrosine with tyramide-Cy5) (Fig. 2B). Further analysis of the colocalization of fibronectin with tyramide-Cy5 showed that fibronectin immunoreactivity correlated closely with the tyrosine analog, tyramide (Fig. 2, C to F; Pearson's correlation of 0.449 and Mander's overlap of 0.909). Similar to these results with immunofluorescence labeling techniques, under the same conditions of fibroblast-derived ECM crosslinking (Fig. 1B), the presence of sodium azide, catalase, DPI, or L-tyrosine inhibited the formation of high MW species of fibronectin catalyzed by MPO and H_2O_2 (fig. S1). These studies demonstrated that susceptible tyrosine residues in fibronectin fibrils on the surface of TGF-β1–differentiated myofibroblasts were catalyzed by MPO to undergo *o,o'*-tyrosine:tyramide crosslinking.

Soluble plasma fibronectin is not susceptible to MPO-mediated o,o'*-dityrosine crosslinking*

Soluble forms of fibronectin, produced primarily in the liver by hepatocytes, are abundant in circulating human plasma and other body fluids (17). Circulating plasma also contains substantial amounts of active MPO (18, 19). Therefore, we determined whether soluble plasma fibronectin was susceptible to *o,o'*-dityrosine crosslinking. The formation of *o,o'*-dityrosine can be detected by the increase in fluorescence at an excitation around 320 nm and emission around 405 nm, indicative of L-tyrosine dimerization (20, 21). Using this method of detection, we found high rates of *o,o'*-dityrosine formation when human soluble plasma fibronectin was incubated with HRP and H_2O_2; in contrast, we were unable to detect *o,o'*-dityrosine formation when MPO was substituted for HRP (Fig. 3A). This restriction on plasma fibronectin oxidative crosslinking was not related to a lack of MPO peroxidative

activity in our assay, because it efficiently catalyzed crosslinking of L-tyrosine (Fig. 3A). To confirm the formation of high MW fibronectin catalyzed by HRP in the presence of H_2O_2, we performed Western blot analyses under reducing conditions. This demonstrated a shift in fibronectin reactivity from ~270 kDa to above 500 kDa, which was not observed with MPO (Fig. 3B). Because soluble fibronectin is in a globular form that may restrict accessibility to susceptible tyrosine residues and cultured cells are able to assemble soluble plasma fibronectin into fibrillar fibronectin on the cell surface (22), we examined if the crosslinking activity of MPO could be recovered by inducing fibrillogenesis of plasma fibronectin. We treated primary mouse fibroblasts with TGF-β1 and then incubated them with human plasma fibronectin in the presence or absence of the hPxs, MPO or HRP. Western blot analysis under reducing conditions, utilizing an antibody (clone IST4) that recognizes only human (but not mouse) fibronectin, demonstrated higher MW species in the presence of MPO or HRP (Fig. 3C). These data support the concept that the selectivity of MPO to catalyze fibronectin *o,o'*-dityrosine crosslinking depended on its three-dimensional conformation, and not necessarily the requirement for extra domain A or B (EDA or EDB), both of which are absent from circulating plasma fibronectin.

Fibronectin o,o'*-dityrosine crosslinking confers protease resistance*

Next, we determined the potential physiological or pathobiological consequences of fibronectin *o,o'*-dityrosine crosslinking. Remodeling of the ECM and eventual reabsorption of matrix molecules during the resolution phase of wound repair depends on the degradation of the ECM by proteases. We tested the effect of oxidative fibronectin *o,o'*-dityrosine crosslinking on the susceptibility to protease activity. First, TGF-β1–activated human lung myofibroblasts that generate endogenous H_2O_2 were incubated with MPO or HRP for 24 hours and then treated with either Proteinase K, which cleaves with broad specificity at the carboxyl side of aliphatic and aromatic amino acids, or the serine proteases, trypsin and plasmin, both of which cleave at the carboxyl side of lysine and arginine residues, prior to SDS-PAGE under reducing conditions and immunoblotting for fibronectin. All three proteases induced a loss of native fibronectin at the expected MW (~270 kDa) with degradation products between 55–200 kDa (Fig. 4, A to C). However, in the presence of hPxs, higher MW species of fibronectin were retained (Fig. 4, A to C), indicating resistance to protease degradation under conditions of fibronectin oxidative crosslinking. These data support that *o,o'*-dityrosine crosslinking of fibonectin within the pericellular matrix acquired resistance to proteolysis, which may contribute to impaired ECM turnover.

Cellular migration is inhibited by o,o'*-dityrosine fibronectin crosslinking*

Cellular migration in embryogenesis, morphogenesis, and wound healing depends on cell-ECM interactions, with a critical role for fibronectin (23). We reasoned that fibronectin *o,o'*-dityrosine crosslinking could alter fibronectin-dependent cellular migration and used a transwell migration assay to test this hypothesis. In the upper chamber of a two-chamber transwell system, we cultured human lung fibroblasts under conditions of native matrix production and *o,o'*-dityrosine crosslinking. After lysing the cells to generate cell-free matrices, a defined number of fibroblasts were seeded onto the matrices in the upper chamber (Fig. 4D). Fibroblast migration through the matrices was decreased when matrices

were generated under conditions of oxidative *o,o'*-dityrosine crosslinking with either HRP or MPO (Fig. 4, E and F).

To further study the effects of crosslinked fibronectin on cell behavior, we tested the effects of plasma fibronectin subjected to chemical crosslinking on fibroblast migration (fig. S2A). As previously reported, we observed an increase in fibroblast migration in the presence of plasma fibronectin (23). However, fibroblast migration was markedly inhibited when plasma fibronectin was modified by *o,o'*-dityrosine crosslinking (fig. S2, B and C). Because epithelial cell migration is thought to be particularly important in wound healing and is dependent on a "provisional" matrix containing fibronectin, we studied the effects of native and oxidatively crosslinked fibronectin on epithelial cell migration using a variation on an in vitro wound healing assay in which the cells were tested for their ability to migrate over a decellularized matrix (Fig. 4G). Wound closure was decreased under conditions of oxidative *o,o'*-dityrosine crosslinking with either HRP or MPO (Fig. 4, H and I). These data support the concept that, in addition to acquired protease resistance, posttranslational modification of fibronectin by *o,o'*-dityrosine disrupts cellular migration.

Fibronectin-associated o,o'*-dityrosine concentrations are increased in lung tissue and plasma in a murine model of lung injury*

From the in vitro evidence that fibronectin was susceptible to crosslinking, we determined if *o,o´*-dityrosine oxidative modifications of fibronectin occurred in vivo. Fibronectin modified by *o,o*'-dityrosine was increased in lung tissue (Fig. 5A) and plasma (Fig. 5B) of mice during the fibrogenic phase of bleomycin-induced lung injury. In whole lung tissue, the average natural log–transformed concentrations of fibronectin *o,o´*-dityrosine in bleomycin-injured mice and controls were 5.19 ± 0.88 and 2.28 ± 0.34 μmol/mol, respectively, corresponding to a 18.36-fold increase on a linear scale. In plasma, fibronectin *o,o´*-dityrosine concentrations increased by 5.58-fold on a linear scale (2.82 ± 1.08 vs. 1.1 ± 1.14 μmol/mol in bleomycin vs. control, respectively, in natural log–transformed data). These data suggest that fibronectin modification by *o,o'*-dityrosine crosslinking occurs during experimental fibrosis in a murine model of lung injury.

Fibronectin-associated o,o'*-dityrosine concentrations are increased in circulating plasma of human subjects with ILD*

ILD is characterized by the progressive loss of normal tissue architecture due to alterations in the ECM that may perpetuate aberrant repair responses to tissue injury (24). We previously reported that total concentrations of *o,o´*-dityrosine are increased in the plasma of patients with ILD (25). Here, we determined whether fibronectin-specific *o,o'*-dityrosine moieties were detectable in human plasma. Fibronectin modified by *o,o'*-dityrosine was increased in the plasma of ILD patients [12 with idiopathic pulmonary fibrosis (IPF) and 4 with connective tissue disease–associated ILD (CTD-ILD)] in comparison to 20 healthy controls (Fig. 5C). Both groups were well matched for age (healthy = 54.8 ± 6.96 μmol/mol, ILD = 55.1 ± 8.29 μmol/mol) and gender [m:f; 3:17 (healthy) and 3:13 (ILD)]. Human subjects with ILD demonstrated a 7.38 fold increase on a linear scale in comparison to healthy subjects (average natural log–transformed fibronectin *o,o´*-dityrosine concentrations: 2.06 ± 1.06 vs. 0.061 ± 0.48 μmol/mol, respectively). These data indicate that fibronectin

modified by *o,o'*-dityrosine crosslinking is detectable in circulating plasma and increased in human subjects with ILD.

DISCUSSION

In this study, we demonstrated that fibronectin was susceptible to oxidation by hPx-catalyzed *o,o'*-dityrosine crosslinking. The steady-state concentrations fibronectin bearing this oxidative modification were increased in the plasma of human subjects with ILD and in both lung tissues and plasma of mice subjected to fibrogenic lung injury. Biochemical characterization of fibronectin oxidative crosslinking demonstrated the formation of fibronectin multimers on SDS-PAGE gels under reducing conditions, supporting the formation of stable, covalent *o,o'*-dityrosine bonds. Cellular signaling by the fibrogenic cytokine, TGF-β1, in lung fibroblasts activates the endogenous production of H_2O_2 by a flavoenyzme that we have previously characterized to be a member of the NADPH oxidase family (26), and promoted fibronectin multimerization in the presence of physiologic concentrations of a mammalian hPx, MPO. Fibronectin crosslinked by *o,o'*-dityrosine was resistant to degradation by multiple proteases, including the broad-spectrum protease Proteinase K. Additionally, fibronectin oxidative crosslinking disrupted fibroblast and epithelial cell migration, in comparison to cellular migration on native, non-crosslinked fibrillar fibronectin.

Fibronectin plays a central role in physiologic and pathologic wound healing (27). It is tyrosine-rich and an important structural and functional contributor to cellular growth, migration, adhesion, differentiation, and survival (17). Fibronectin is essential in the dynamic, tightly regulated repair processes that follow tissue injury, wherein it is a critical component of the provisional matrix and orchestrates reepithelialization (28, 29). The modification of fibronectin by *o,o'*-dityrosine, a kinetically favorable reaction in the oxidative and inflammatory environment of the healing wound, could be envisioned to play an important role in the normal physiologic wound healing process. The capacity for the mammalian hPx, MPO, to mediate *o,o'*-dityrosine crosslinking of fibronectin appeared to require cell-dependent fibrillogenesis, suggesting that there may be cryptic sites containing tyrosine residues that are susceptible to oxidation only when the protein is in its fibrillar form and offering an explanation for why circulating plasma fibronectin was protected from this posttranslational modification. Unlike reversible cysteine oxidation, mechanisms for the reversibility of *o,o'*-dityrosine bonds are not known. It is possible that proteases present in the milieu of resolving wounds are sufficient to generate fragments that may then be taken up by the circulation and excreted by the kidneys. This possibility is supported by our finding of higher quantities of circulating *o,o'*-dityrosine fragments in both human subjects with lung disease and animal models of lung injury-fibrosis.

The formation of *o,o'*-dityrosine may be favored in pathologic states in which there are high concentrations of H_2O_2 and an hPx capable of catalyzing this reaction. This is certainly true in aging, wherein oxidant-antioxidant imbalance contributes to higher concentrations of H_2O_2 and non-resolving fibrosis (30). Indeed, the formation of *o,o'*-dityrosine has been reported to be a biomarker of aging (31). Prior reports of *o,o'*-dityrosine formation in human tissues have involved age-related pathologies, including atherosclerosis (32, 33),

neurodegeneration (34, 35), and cataracts (36). Based on our data that *o,o'*-dityrosine modification of fibronectin rendered this protein resistant to proteolysis, we speculate that such oxidatively crosslinked proteins accumulate over time in chronic diseases of aging, including IPF, that may represent aberrant wound healing responses.

Our studies indicate that *o,o'*-dityrosine modification of fibronectin altered its signaling and/or structural properties in a manner that limited cellular migration. This alteration may interfere with normal reepithelialization, a common feature of non-resolving wounds that culminate in fibrosis (37). When further analyzing the tyrosine content in fibronectin, tyrosine enrichment is present within the 70 kDa migration stimulation factor region of the protein containing type I and II repeats (5.14%; 33 tyrosines:642 amino acids; Uniprot #PO2751–2). Our data on alterations in fibroblast migration suggest that tyrosines in this region may be oxidized. Future studies will identify the specific tyrosine residues within fibronectin that are susceptible to tyrosyl radical formation and *o,o'*-dityrosine crosslinking. Although our studies clearly implicate fibronectin as a target of *o,o'*-dityrosine oxidation, it is possible that other ECM proteins are also susceptible to this oxidative modification. We think such modifications are relatively minor in comparison based on our ex vivo fibroblast system in which an unbiased approach to identifying proteins that link to a tyrosine analog (tyramide) demonstrated only two fairly distinct bands, one at the expected MW of fibronectin and another at approximately 125–140 kDa, the identity of which is yet to be determined.

In summary, we report the oxidative crosslinking of the ECM protein fibronectin by *o,o'*-dityrosine bonding that is catalyzed by a hPx in an H_2O_2-dependent manner. Wound healing microenvironments in the lung and other organ systems characterized by high steady-state concentrations of H_2O_2 and a pro-inflammatory milieu are permissive to these oxidative reactions, which may contribute to the non-resolving pathology in age-related neurodegenerative, atherosclerotic, and fibrotic disorders.

MATERIALS AND METHODS

Cell culture

Human fetal lung fibroblasts (IMR-90, Coriell Institute for Medical Research) and human lung epithelial cells (A549, ATCC) were grown in Dulbecco's Modification of Eagle's Medium (Catalog # 15–013-CM; Corning) supplemented with 10% fetal bovine serum, 2 mM L-glutamine, 100 units/ml penicillin, 100 μg/ml streptomycin, and 1.25 μg/ml fungizone (Gibco). Cells were grown at 37°C in 5% CO_2. At 90% confluence, cells were placed in serum free medium for 24 hrs prior to stimulation with porcine TGF-β1 (2 ng/mL; Catalog # 101-B1; R&D System) to stimulate differentiation into myofibroblasts and induce H_2O_2 production (maximal at 16 hr). Cells were treated with HRP (5 U/mL; Catalog # P8375; Sigma-Aldrich) or MPO from human leukocytes (5 U/mL; Catalog # M6908; Sigma-Aldrich). Myofibroblasts were also treated with peritoneal PMNs isolated from littermate control $Mpo^{+/+}$ and $Mpo^{-/-}$ mice as previously described (38). In the inhibitor studies, fibroblasts were pretreated for 15 mins with sodium azide (1 mM; Catalog # 71289; all four inhibitors from Sigma Aldrich), Catalase (3000 U/mL; Catalog # C1345), DPI (10 μM; Catalog # D2926), or L-tyrosine (5 mM; Catalog # 93829) prior to addition of MPO.

Western blotting and antibodies

Total cell lysates were prepared in boiling 1% SDS lysis buffer (10 mM Tris, pH 7.4) supplemented with protease inhibitors, followed by BCA assay, and addition of NuPAGE reducing agent and NuPAGE LDS sample buffer (Catalog # NP0009 and NP0007; Invitrogen Corp) with SDS-PAGE electrophoresis performed. For neutravidin pull down experiments NeutrAvidin Agarose (Catalog # 29200; Thermo Fisher Scientific) was utilized. For protease experiments, after hPx treatment for 24 hours the cells were treated with either Proteinase K (Catalog # P6556; Sigma Aldrich), trypsin (Catalog # SH30042.01; Thermo Fisher Scientific), or plasmin (Catalog # P1867; Sigma Aldrich) and SDS-PAGE electrophoresis was immediately performed. Antibodies to human fibronectin (1:500; clone IST4, mouse monoclonal that recognizes an epitope located within the fifth type III repeat of human fibronectin; Catalog # F0916, Sigma Aldrich), fibronectin (1:500; clone IST9, mouse monoclonal that recognizes an epitope (PEDGIHELFP) located in the EDA sequence of cellular fibronectin; Catalog # sc-59826 AC, Santa Cruz Biotechnology), and β-actin (1:10,000; clone AC-15, mouse mAb against N-terminal peptide; Catalog # A1978; Sigma Aldrich) were utilized. Secondary antibody goat anti-mouse IgG (H+L) cross absorbed antibody conjugated to HRP (Catalog # 31432; Thermo Scientific) was used for detection by chemiluminescence. Immunoblots were imaged using an Amersham Biosciences 600 Imager and analyzed with TotalLab (GE Healthcare).

Tyramide-crosslinked tyrosine labeling

We have previously described a fluorescent labeling technique to detect hPx-catalyzed, H_2O_2-mediated crosslinking of tyrosine residues on endogenous protein substrates (9). Briefly, tyramide, a tyrosine analogue, conjugated to biotin or Cy5 (PerkinElmer) is utilized to label protein tyrosine residues susceptible to *o,o'*-biphenolic covalent linkage. After treatment with or without TGF-β1 for 16 hrs, biotin-tyramide or tyramide-Cy5 is incubated in the presence/absence of MPO for 4 hrs in serum free medium. For studies utilizing biotin-tyramide, protein lysates subjected were probed with streptavidin directly conjugated to HRP and visualized with chemiluminescence. Lysates from biotin-tyramide - treated fibroblasts were then subjected to purification utilizing Neutravidin Plus Ultralink Resin (Catalog # 53151; Pierce). For studies utilizing tyramide-Cy5, fibroblasts were fixed with 4% paraformaldehyde and probed with human fibronectin (1:500; clone IST4), secondary antibody Cy2 AffiniPure Donkey anti-mouse IgG (1:100; Catalog # 715–225-150; Jackson ImmunoResearch Laboratories), and stained with Hoechst 33342 trihydrochloride trihydrate (Catalog # H3570; Thermo Fisher Scientific).

Microscopy

Digital images were acquired using the Keyence BZ-X700 All-in-one microscope. A PlanFluor 40x NA 0.60/3.60–2.80 Ph2 objective was used for the digital fluorescent images, and a CFI PlanApo λ 2 × 0.10/8.50 mm objective was used to capture the crystal violet stained transwell and wound healing assay images. For fluorescent images BZX GFP (OP-87763), BZX Cy5 (OP-87766), and BZX DAPI (OP-87762) filters were used. BZ-X Viewer was used for image capture. Confocal images were acquired using the Nikon A1R

Confocal Imaging System. An Apo 60x Oil λS DIC N2 objective and 405nm, 488nm, 561nm laser lines used. Nis Elements 5.02 was used for image capture and adjustments.

Plasma fibronectin *o,o*-dityrosine

Purified human plasma fibronectin (Catalog # F2006; Sigma-Aldrich, St. Louis, MO) was treated with or without H_2O_2 (Catalog # H1009; Sigma-Aldrich, St. Louis, MO) in the presence or absence of HRP and MPO. Fluorescence intensity of *o,o'*-dityrosine formation was measured in a kinetic assay with the BioTek Synergy Mx system (BioTek Instruments, Winooski, VT) utilizing Gen5 2.05 software at the excitation wavelength of 320 nm and emission of 405 nm. Mouse lung fibroblasts were isolated from male C57BL/6 as previously described (39). Human plasma fibronectin and MPO (5 U/mL) was added to TGF-β1 (4 ng/mL)-stimulated fibroblasts. Total mouse lung lysate was collected in boiling 1% SDS lysis buffer and subjected to western blot analysis under reducing conditions.

Cellular migration assays and isolation of cell-derived matrices

Human lung fibroblasts were cultured on transparent PET membrane cell culture inserts (24 well, 8.0 μm pore size; Catalog # 353097; Falcon), treated with TGF-1 (2 ng/mL) and a hPx (5 U/mL MPO or HRP), and matrix isolation performed. Matrix isolation was carried out as previously described (40). Briefly, extraction buffer (20 mM NH_4OH, 0.5% (v/v) Triton X-100 in PBS, pH 7.4) was gently added to the culture plates, upon cellular detachment matrix was washed twice with PBS and treated with DNase (10 U/mL; Catalog # EN0521; Thermo Fisher Scientific) for 1 hr followed by two PBS washes prior to subsequent migration experiments. The same conditions were utilized for fibroblast matrix formation and isolation for the epithelial cell wound healing assay that utilized 2 well culture inserts (Catalog # 80209; Ibidi).

Mice and human subjects

Intratracheal bleomycin (1.25 U/kg) was administered to induce lung injury or saline (50 μL total volume) to two-month-old female C57BL/6 mice (The Jackson Laboratory, Bar Harbor, ME) as previously described(26). Three weeks post injury mice were sacrificed by CO_2 inhalation, and lung tissue and plasma collected. Plasma samples were collected from 16 human subjects with ILD (12 IPF, 4 CTD-ILD) and from 20 healthy control subjects matched for age (healthy = 54.8 ± 6.96, ILD = 55.1 ± 8.29) and gender [m:f; 3:17 (healthy) and 3:13(ILD)]. All procedures involving animals and human subjects were approved by the Institutional Animal Care and Use Committees and Institutional Review Boards at the University of Alabama at Birmingham and the University of Michigan.

Mass spectrometry analysis

Fibronectin was immunoprecipitated from lung tissue or plasma using anti-fibronectin antibody. Samples were then analyzed as previously outlined(41). In short, protein was precipitated with ice-cold trichloroacetic acid (10% v/v) from the fibronectin immunoprecipitated lung tissue or plasma samples and diluted in 50 mM phosphate buffer pH 7.4. The protein precipitate was delipidated with water/methanol/water-washed diethyl ether (1:3:7; v/v/v). Known concentrations of isotopically labeled internal standards $^{13}C_6$

tyrosine or $^{13}C_{12}$ *o,o´*-dityrosine were added, and samples were hydrolyzed for 24 hrs in 4 N methane sulfonic acid treated with benzoic acid. Oxidized amino acids were cleaned using Superclean ENVI ChromP columns (3ml, Supelco Inc., Bellefonte, PA). Oxidized amino acids were quantified by liquid chromatography-electrospray ionization tandem mass spectrometry (LC-ESI-MS/MS) with multiple reaction monitoring (MRM) MS/MS positive ion acquisition mode utilizing an Agilent 6410 triple quadrupole MS system equipped with an Agilent 1200 LC system. Labeled precursor amino acid, $^{13}C_9{}^{15}N_1$tyrosine, was added to monitor potential internal artifact formation of *o,o´*-dityrosine and was noted to be negligible.

Data analysis

Student unpaired t test was used to compare the natural log-transformed data between groups in the murine and human studies. One-way ANOVA with post hoc Tukey's was used to compare groups in the in vitro studies. P values less than or equal to 0.05 were considered significant. Analyses and graphs were generated using GraphPad Prism version 6.00 (GraphPad Software, La Jolla, CA, USA). Error bars in figures represent group mean ± standard deviation (SD).

Supplementary Material

Refer to Web version on PubMed Central for supplementary material.

Acknowledgments:

Confocal imaging was performed in the UAB High Resolution Imaging Facility Service Center with the help of Shawn Williams.

Funding:

This study was supported by NIH grants, R01 AG046210 and P01 HL114470 (to VJT), R01 HL139617 (to JWZ and VJT), and F30 HL136195 (to MLL), and a Department of Veteran's Affairs Merit Award I01BX003056 (to VJT). The authors declare no competing financial interests.

Data and Materials Availability:

The mass spectrometry data have been deposited into the Mass Spectrometry Interactive Virtual Environment (MassIVE) database, https://massive.ucsd.edu/ProteoSAFe/static/massive.jsp, with the identifier MSV000085451. All other data needed to evaluate the conclusions in the paper are present in the paper or the Supplementary Materials.

REFERENCES AND NOTES

1. Thannickal VJ, and Fanburg BL 2000. Reactive oxygen species in cell signaling. American journal of physiology. Lung cellular and molecular physiology 279: L1005–1028. [PubMed: 11076791]
2. Lyles MM, and Gilbert HF 1994. Mutations in the thioredoxin sites of protein disulfide isomerase reveal functional nonequivalence of the N- and C-terminal domains. The Journal of biological chemistry 269: 30946–30952. [PubMed: 7983029]
3. Stadtman ER, and Levine RL 2000. Protein oxidation. Annals of the New York Academy of Sciences 899: 191–208. [PubMed: 10863540]

4. Anh NT, Nishitani M, Harada S, Yamaguchi M, and Kamei K. 2011. Essential role of Duox in stabilization of Drosophila wing. The Journal of biological chemistry 286: 33244–33251. [PubMed: 21808060]
5. Kumar S, Molina-Cruz A, Gupta L, Rodrigues J, and Barillas-Mury C. 2010. A peroxidase/dual oxidase system modulates midgut epithelial immunity in Anopheles gambiae. Science 327: 1644–1648. [PubMed: 20223948]
6. Wong JL, and Wessel GM 2009. Extracellular matrix modifications at fertilization: regulation of dityrosine crosslinking by transamidation. Development 136: 1835–1847. [PubMed: 19403662]
7. Edens WA, Sharling L, Cheng G, Shapira R, Kinkade JM, Lee T, Edens HA, Tang X, Sullards C, Flaherty DB, Benian GM, and Lambeth JD 2001. Tyrosine cross-linking of extracellular matrix is catalyzed by Duox, a multidomain oxidase/peroxidase with homology to the phagocyte oxidase subunit gp91phox. The Journal of cell biology 154: 879–891. [PubMed: 11514595]
8. Wong JL, and Wessel GM 2008. Free-radical crosslinking of specific proteins alters the function of the egg extracellular matrix at fertilization. Development 135: 431–440. [PubMed: 18094022]
9. Larios JM, Budhiraja R, Fanburg BL, and Thannickal VJ 2001. Oxidative protein cross-linking reactions involving L-tyrosine in transforming growth factor-beta1-stimulated fibroblasts. The Journal of biological chemistry 276: 17437–17441. [PubMed: 11279068]
10. Zhou Y, Horowitz JC, Naba A, Ambalavanan N, Atabai K, Balestrini J, Bitterman PB, Corley RA, Ding BS, Engler AJ, Hansen KC, Hagood JS, Kheradmand F, Lin QS, Neptune E, Niklason L, Ortiz LA, Parks WC, Tschumperlin DJ, White ES, Chapman HA, and Thannickal VJ 2018. Extracellular matrix in lung development, homeostasis and disease. Matrix Biol.
11. Siegel RC, Pinnell SR, and Martin GR 1970. Cross-linking of collagen and elastin. Properties of lysyl oxidase. Biochemistry 9: 4486–4492. [PubMed: 5474144]
12. Kornguth SE, and Waelsch H. 1963. Protein modification catalysed by transglutaminase. Nature 198: 188–189. [PubMed: 14034831]
13. Thannickal VJ, and Fanburg BL 1995. Activation of an H2O2-generating NADH oxidase in human lung fibroblasts by transforming growth factor beta 1. The Journal of biological chemistry 270: 30334–30338. [PubMed: 8530457]
14. Arnhold J, and Flemmig J. 2010. Human myeloperoxidase in innate and acquired immunity. Archives of biochemistry and biophysics 500: 92–106. [PubMed: 20399194]
15. Nauseef WM 2014. Myeloperoxidase in human neutrophil host defence. Cell Microbiol 16: 1146–1155. [PubMed: 24844117]
16. Tien M. 1999. Myeloperoxidase-catalyzed oxidation of tyrosine. Archives of biochemistry and biophysics 367: 61–66. [PubMed: 10375399]
17. Pankov R, and Yamada KM 2002. Fibronectin at a glance. J Cell Sci 115: 3861–3863. [PubMed: 12244123]
18. Zhang R, Shen Z, Nauseef WM, and Hazen SL 2002. Defects in leukocyte-mediated initiation of lipid peroxidation in plasma as studied in myeloperoxidase-deficient subjects: systematic identification of multiple endogenous diffusible substrates for myeloperoxidase in plasma. Blood 99: 1802–1810. [PubMed: 11861298]
19. Bradley PP, Christensen RD, and Rothstein G. 1982. Cellular and extracellular myeloperoxidase in pyogenic inflammation. Blood 60: 618–622. [PubMed: 6286012]
20. Heinecke JW, Li W, Francis GA, and Goldstein JA 1993. Tyrosyl radical generated by myeloperoxidase catalyzes the oxidative cross-linking of proteins. The Journal of clinical investigation 91: 2866–2872. [PubMed: 8390491]
21. Cheng G, Li H, Cao Z, Qiu X, McCormick S, Thannickal VJ, and Nauseef WM 2011. Vascular peroxidase-1 is rapidly secreted, circulates in plasma, and supports dityrosine cross-linking reactions. Free radical biology & medicine 51: 1445–1453. [PubMed: 21798344]
22. Singh P, Carraher C, and Schwarzbauer JE 2010. Assembly of fibronectin extracellular matrix. Annu Rev Cell Dev Biol 26: 397–419. [PubMed: 20690820]
23. Clark RA, An JQ, Greiling D, Khan A, and Schwarzbauer JE 2003. Fibroblast migration on fibronectin requires three distinct functional domains. J Invest Dermatol 121: 695–705. [PubMed: 14632184]

24. Kulkarni T, de Andrade J, Zhou Y, Luckhardt T, and Thannickal VJ 2016. Alveolar epithelial disintegrity in pulmonary fibrosis. American journal of physiology. Lung cellular and molecular physiology 311: L185–191. [PubMed: 27233996]
25. Pennathur S, Vivekanandan-Giri A, Locy ML, Kulkarni T, Zhi D, Zeng L, Byun J, de Andrade JA, and Thannickal VJ 2015. Oxidative Modifications of Protein Tyrosyl Residues are Increased in Plasma of Human Subjects with Interstitial Lung Disease. American journal of respiratory and critical care medicine.
26. Hecker L, Vittal R, Jones T, Jagirdar R, Luckhardt TR, Horowitz JC, Pennathur S, Martinez FJ, and Thannickal VJ 2009. NADPH oxidase-4 mediates myofibroblast activation and fibrogenic responses to lung injury. Nature medicine 15: 1077–1081.
27. To WS, and Midwood KS 2011. Plasma and cellular fibronectin: distinct and independent functions during tissue repair. Fibrogenesis & tissue repair 4: 21. [PubMed: 21923916]
28. Wierzbicka-Patynowski I, and Schwarzbauer JE 2002. Regulatory role for SRC and phosphatidylinositol 3-kinase in initiation of fibronectin matrix assembly. The Journal of biological chemistry 277: 19703–19708. [PubMed: 11912200]
29. Lenselink EA 2015. Role of fibronectin in normal wound healing. Int Wound J 12: 313–316. [PubMed: 23742140]
30. Hecker L, Logsdon NJ, Kurundkar D, Kurundkar A, Bernard K, Hock T, Meldrum E, Sanders YY, and Thannickal VJ 2014. Reversal of persistent fibrosis in aging by targeting Nox4-Nrf2 redox imbalance. Science translational medicine 6: 231ra247.
31. Feeney MB, and Schoneich C. 2012. Tyrosine modifications in aging. Antioxidants & redox signaling 17: 1571–1579. [PubMed: 22424390]
32. Leeuwenburgh C, Rasmussen JE, Hsu FF, Mueller DM, Pennathur S, and Heinecke JW 1997. Mass spectrometric quantification of markers for protein oxidation by tyrosyl radical, copper, and hydroxyl radical in low density lipoprotein isolated from human atherosclerotic plaques. The Journal of biological chemistry 272: 3520–3526. [PubMed: 9013599]
33. Francis GA, Mendez AJ, Bierman EL, and Heinecke JW 1993. Oxidative tyrosylation of high density lipoprotein by peroxidase enhances cholesterol removal from cultured fibroblasts and macrophage foam cells. Proceedings of the National Academy of Sciences of the United States of America 90: 6631–6635. [PubMed: 8341680]
34. Al-Hilaly YK, Williams TL, Stewart-Parker M, Ford L, Skaria E, Cole M, Bucher WG, Morris KL, Sada AA, Thorpe JR, and Serpell LC 2013. A central role for dityrosine crosslinking of Amyloid-beta in Alzheimer's disease. Acta neuropathologica communications 1: 83. [PubMed: 24351276]
35. Souza JM, Giasson BI, Chen Q, Lee VM, and Ischiropoulos H. 2000. Dityrosine cross-linking promotes formation of stable alpha -synuclein polymers. Implication of nitrative and oxidative stress in the pathogenesis of neurodegenerative synucleinopathies. The Journal of biological chemistry 275: 18344–18349. [PubMed: 10747881]
36. McNamara MK, and Augusteyn RC 1980. 3,3'-Dityrosine in the proteins of senile nuclear cataracts. Exp Eye Res 30: 319–321. [PubMed: 7398812]
37. Thannickal VJ, Toews GB, White ES, Lynch JP 3rd, and Martinez FJ 2004. Mechanisms of pulmonary fibrosis. Annual review of medicine 55: 395–417.
38. Bone NB, Liu Z, Pittet JF, and Zmijewski JW 2017. Frontline Science: D1 dopaminergic receptor signaling activates the AMPK-bioenergetic pathway in macrophages and alveolar epithelial cells and reduces endotoxin-induced ALI. J Leukoc Biol 101: 357–365. [PubMed: 27733575]
39. Barnes JW, Duncan D, Helton S, Hutcheson S, Kurundkar D, Logsdon NJ, Locy M, Garth J, Denson R, Farver C, Vo HT, King G, Kentrup D, Faul C, Kulkarni T, De Andrade JA, Yu Z, Matalon S, Thannickal VJ, and Krick S. 2019. Role of fibroblast growth factor 23 and klotho cross talk in idiopathic pulmonary fibrosis. American journal of physiology. Lung cellular and molecular physiology 317: L141–L154. [PubMed: 31042083]
40. Beacham DA, Amatangelo MD, and Cukierman E. 2007. Preparation of extracellular matrices produced by cultured and primary fibroblasts. Curr Protoc Cell Biol Chapter 10: Unit 10 19.

41. Vivekanandan-Giri A, Byun J, and Pennathur S. 2011. Quantitative analysis of amino Acid oxidation markers by tandem mass spectrometry. Methods in enzymology 491: 73–89. [PubMed: 21329795]

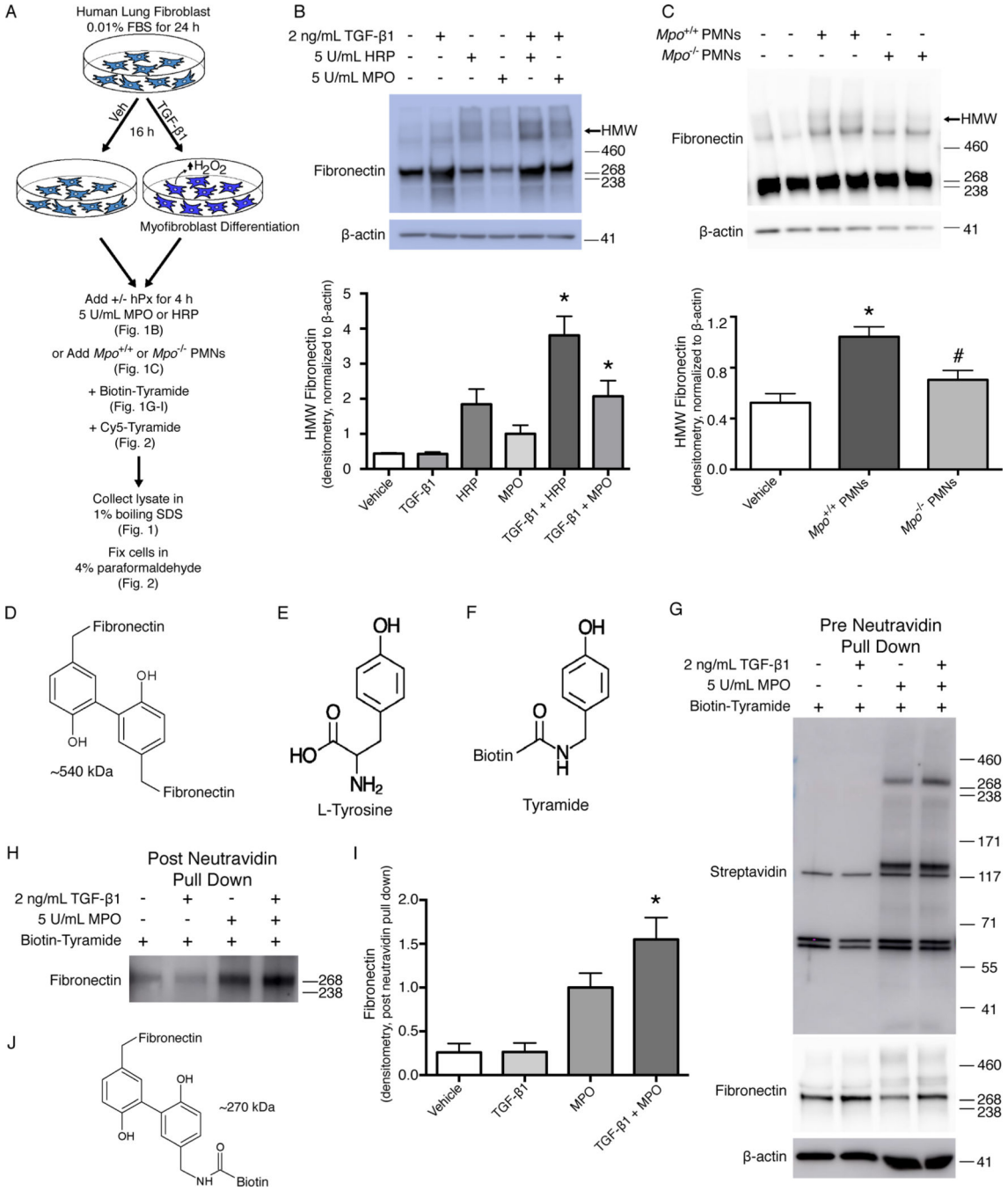

Fig. 1. Tyrosine residues in cellular fibronectin are susceptible to *o,o'*-dityrosine crosslinking.

(**A**) Schematic of the experimental design. Human lung fibroblasts were treated with vehicle (Veh) or TGF-β1 to stimulate differentiation into myofibroblasts and production of H_2O_2. MPO, HRP, or polymorphonuclear leukocytes (PMNs) from $Mpo^{+/+}$ or $Mpo^{-/-}$ mice were added to stimulate oxidation of tyrosine residues in the presence or absence of biotin-tyramide or Cy5-tyramide. (**B, C**) Western blot analysis of fibronectin (B) and quantification of high-molecular weight (HMW) fibronectin (C) in lysates from fibroblasts treated as indicated. β-actin is a loading control. Positions of MW standards are indicated to

the right of the blot. Data show the mean ± SD; $n = 4$ independent experiments; * $p \leq 0.05$ compared to treatment with TGF-β1 alone. ANOVA with post hoc Tukey's. (**D, E**) Western blot analysis of fibronectin (D) and quantification of HMW fibronectin (E) in lysates from fibroblasts treated with PMNs. β-actin is a loading control. Data show the mean ± SD; $n = 6–8$ individual wells from 3 independent experiments. *, $p \leq 0.05$ compared to vehicle; #, $p \leq 0.05$ compared to $Mpo^{+/+}$ PMNs. ANOVA with post hoc Tukey's. (**F**) Structure of putative tyrosine-crosslinked fibronectin homodimers. (**G-H**) Structures of L-tyrosine (G) and biotinylated tyramide (H). (**I**) Western blot analysis of biotin (detected with labelled streptavidin) and fibronectin in lysates from cells treated as indicated. (**J, K**) Western blot analysis (J) and quantification (K) of fibronectin in neutravidin precipitates of cell lysates. Data show mean ± SD; $n = 3$ independent experiments; * $p \leq 0.05$ compared to TGF-β1 alone. ANOVA with post hoc Tukey's. (**L**) Structure of fibronectin crosslinked to biotinylated tyramide.

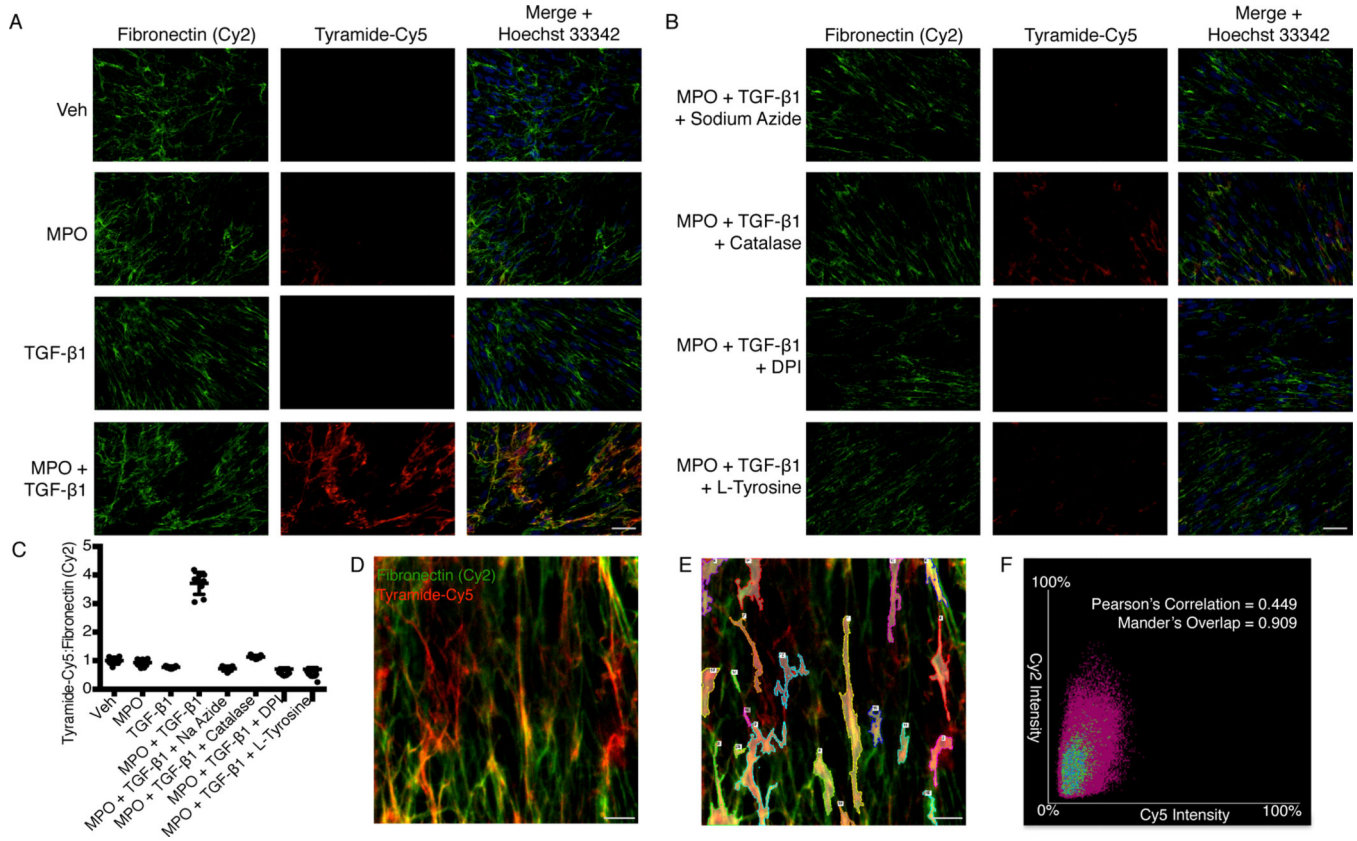

Fig. 2. Colocalization of fibronectin with L-tyrosine analog, tyramide-Cy5.

(**A**) Immunofluorescence images showing fibronectin (detected with a Cy2-labelled secondary antibody) and tyramide-Cy5 in human lung fibroblasts treated with vehicle, MPO, TGF-β1, or MPO + TGF-β1 in the presence of tyramide-Cy5. Images are representative of 3 independent experiments. Scale bar, 50 μm. (**B**) Immunofluorescence images showing fibronectin (Cy2) and tyramide-Cy5 in human lung fibroblasts treated with MPO + TGF-β1 in the presence of tyramide-Cy5 plus sodium azide (an hPx inhibitor), catalase (an hPx competitor), DPI (an inhibitor of H_2O_2 production), or L-tyrosine (a competitor for tyramide-Cy5 binding). Scale bar, 50 μm. (**C**) Ratiometric quantification of tyramide-Cy5 to total fibronectin (Cy2) fluorescence per high power field (hpf) from cells treated as indicated. $n = 9$ total hpf per group from three independent experiments. (**D**) Confocal microscopy showing tyramide-Cy5 and fibronectin (Cy2) in human lung fibroblasts treated with MPO + TGF-β1. Scale bar, 5 μm. (**E**) Same image as in (C) highlighting 20 regions of interest used to perform colocalization analysis of tyramide-Cy5 crosslinking and fibronectin (Cy2). Scale bar, 5 μm. (**F**) Representative scatter plot of Cy5 versus Cy2 intensity in regions highlighted in (E). Pearson's Correlation and Mander's Overlap represents colocalization of Cy5 with Cy2 fluorescence from three independent experiments.

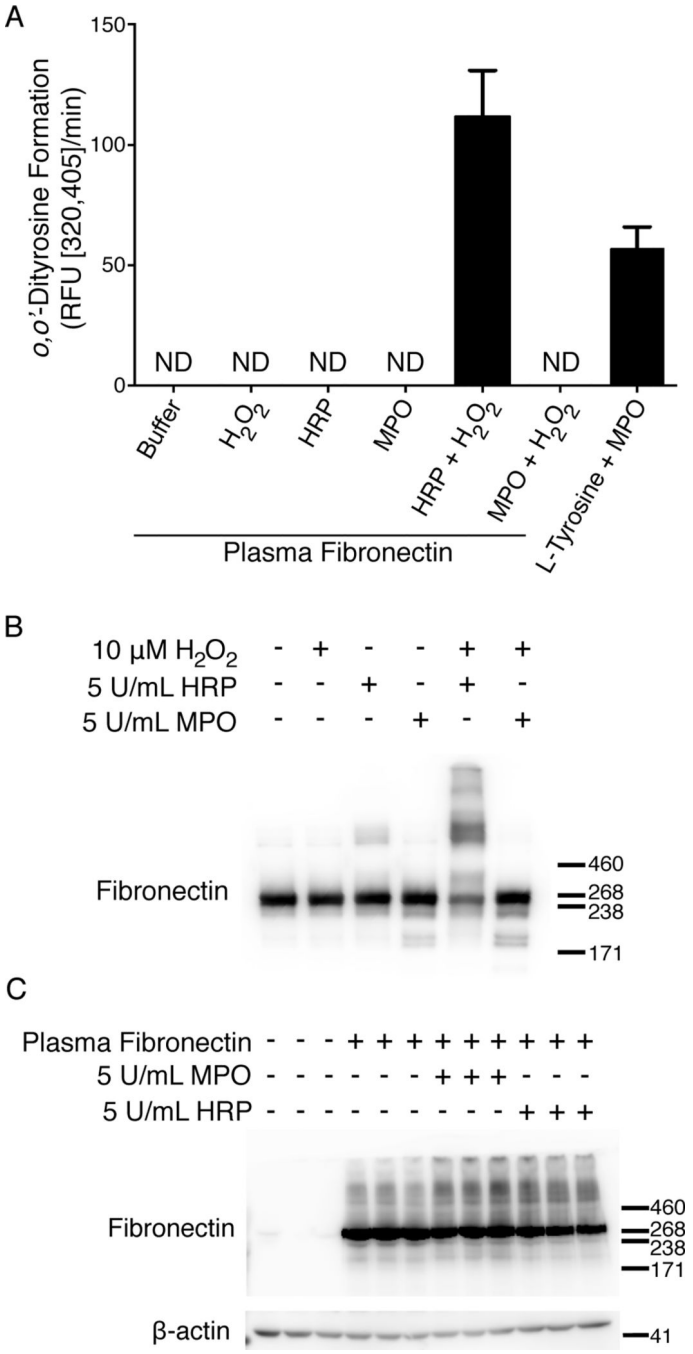

Fig. 3. Plasma fibronectin that undergoes fibrillogenesis is susceptible to MPO-mediated *o,o'*-dityrosine crosslinking.

(**A**) Fluorescence spectroscopy measuring the *o,o'*-dityrosine formation rate of soluble plasma fibronectin treated as indicated. L-tyrosine treatment with MPO and H_2O_2 (L-tyrosine + MPO) was performed as a positive control. Fluorescence was measured at excitation of 320 nm and an emission of 405 nm. ND, not detectable. Data are representative of three independent experiments and show mean ± SD $n = 3$ independent experiments. (**B**) Western blot analysis of soluble, pure plasma fibronectin treated as indicated. The positions

of molecular weight standards are indicated to the right of the blot. Data are representative of three independent experiments. (**C**) Western blot analysis of fibronectin from lysates of mouse lung myofibroblasts that were treated as indicated. β-actin is a loading control. Data are representative of three independent experiments.

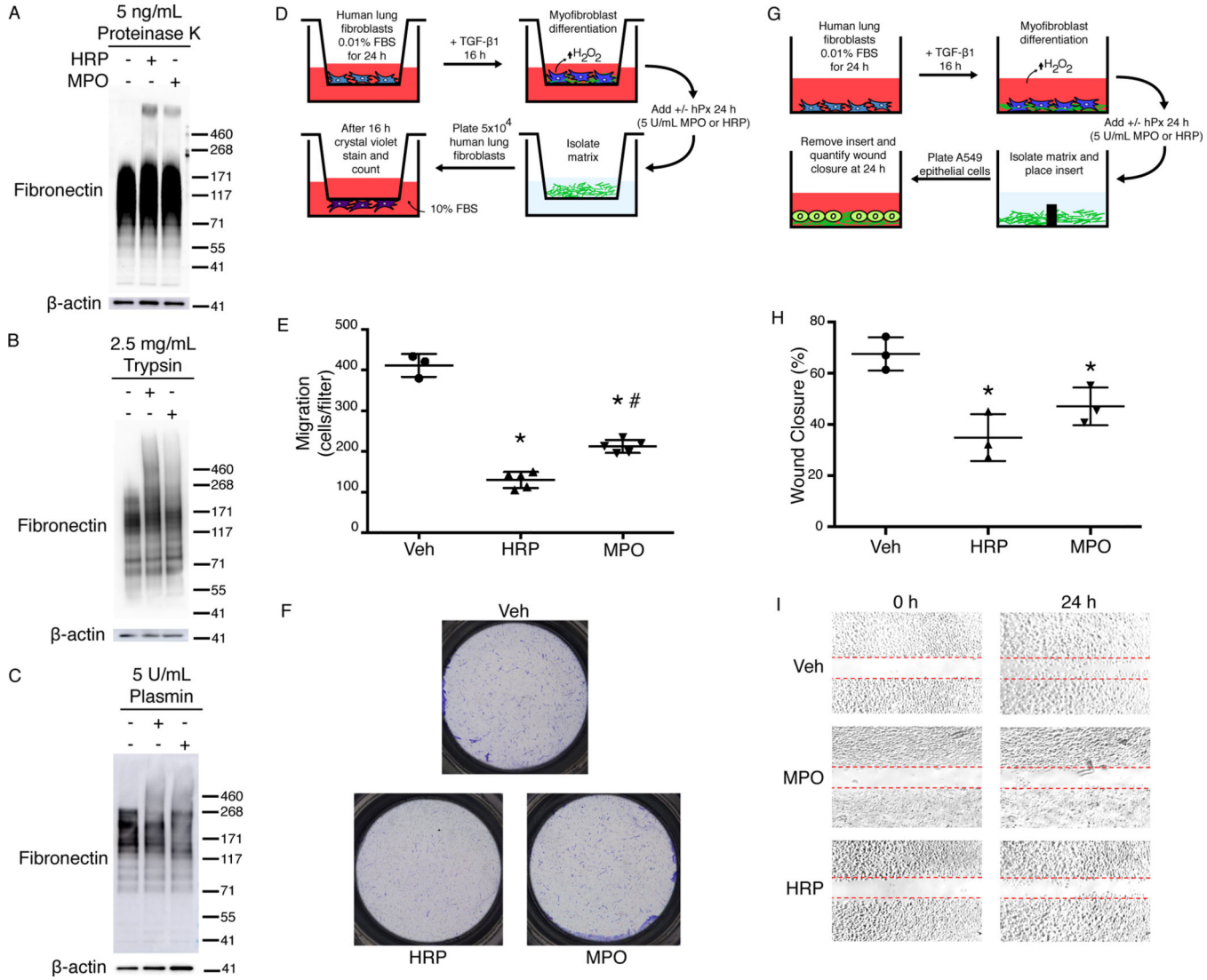

Fig. 4. Fibronectin *o,o'*-dityrosine crosslinking confers protease resistance and inhibits fibroblast and epithelial cell migration.

(**A-C**) Western blot analyses of fibronectin in lysates from human lung myofibroblasts treated with the indicated proteases. β-actin is a loading control. Data are representative of three independent experiments. The positions of molecular weight standards are indicated to the right of the blot. (**D**) Schematic of the experimental design of the transwell migration assay. Human lung fibroblasts in the upper chamber were treated with TGF-β1 to stimulate differentiation into myofibroblasts and H_2O_2 production. MPO or HRP (hPx) was added to stimulate oxidation of tyrosine residues, then the matrix was decellularized. Fibroblasts were then plated on the decellularized matrix and tested for migration through the matrix into the lower chamber. (**E**) Total number of fibroblasts that migrated to the bottom of the transwell. Data show mean ± SD; *n* = three independent experiments with 3–5 transwell inserts per experiment. * indicates significantly decreased fibroblast migration compared to vehicle control (Veh); # indicates significantly increased migration compared to HRP. $P < 0.05$. ANOVA with post hoc Tukey's. (**F**) Images of crystal violet–stained cells after fibroblast

migration to the bottom of the transwell. Data are representative of three independent experiments. (**G**) Schematic of the experimental design of the wound healing assay. Human lung fibroblasts were treated with TGF-β1 to stimulate differentiation into myofibroblasts and H_2O_2 production. MPO or HRP were added to stimulate oxidation of tyrosine residues. After the matrix was decellularized, an insert was added to divide the chamber, and lung epithelial cells were plated on each side of the insert. After cells attained confluence, the inserts were removed and the cells were imaged at 0 and 24 h. (**H**) Percentage of wound closure that occurred at 24 h normalized 0 h. Data show mean ± SD compared to Veh control. $n = 3$ independent experiments with 3 technical replicates per experiment. * indicates significantly decreased epithelial cell wound closure compared to Veh. $P < 0.05$, ANOVA with post hoc Tukey's. (**I**) Images of epithelial cell wound closure on matrices isolated from fibroblasts that were treated with vehicle, MPO, or HRP. Dashed red lines indicate the original gap in the epithelial layer resulting from removing the well insert. Data are representative of 3 independent experiments.

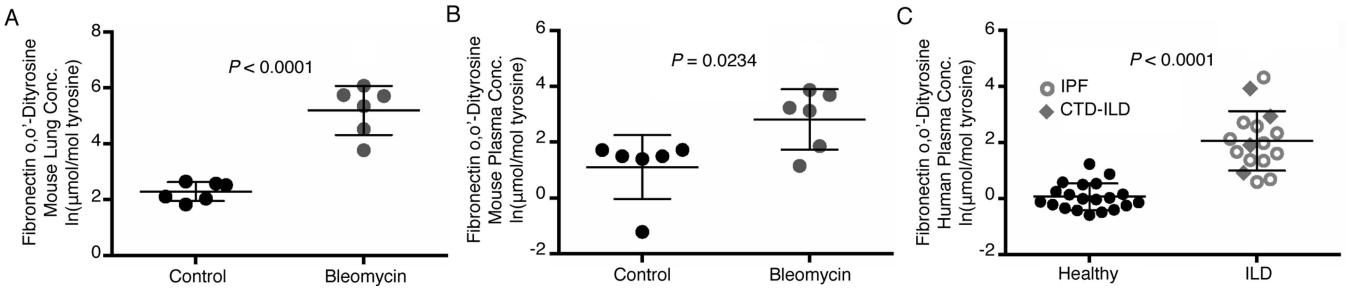

Fig. 5. Fibronectin-associated *o,o'*-dityrosine concentrations are increased in a murine model of lung fibrosis and in ILD patients.

(**A**-**B**) Mass spectrometry analysis of fibronectin-associated *o,o'*-dityrosine concentrations in the lung tissue (A) and plasma (B) from control (saline-treated) and bleomycin-treated mice during the fibrogenic phase (3 weeks after bleomycin injury. Data show mean ± SD; natural log–transformed. $n = 6$ mice in each treatment group. $P < 0.05$, unpaired t test.

(**C**) Mass spectrometry analysis of fibronectin-associated *o,o'*-dityrosine concentrations in plasma from human subjects with IPF or CTD-ILD and age- and sex-matched healthy control subjects. Data show mean ± SD; natural log–transformed. $n = 16$–20 patients per group. $P < 0.05$, unpaired t-test.

Table 1.

Tyrosine Content of Human Extracellular Matrix Proteins

Matrix Molecule	Number of Tyrosine Residues	Total Number of Amino Acids	Percent Tyrosine	UniProt Number
Fibronectin	100	2386	4.19	P02751
Collagen XII, α1	113	3063	3.69	Q99715
Fibrillin 1	93	2871	3.24	P35555
Tenascin-C	66	2201	3.00	P24821
Tenascin-X	119	4242	2.81	P22105
Thrombospondin 1	31	1170	2.65	P07996
Perlecan	109	4391	2.48	P98160
Laminin, α5	88	3695	2.38	015230
SPARC	7	303	2.31	P09486
Elastin	15	786	1.91	P15502
Collagen IV, α2	28	1712	1.64	P08572
Agrin	29	2067	1.4	000468
Collagen IV, α1	18	1669	1.08	P02462
Collagen III, α1	15	1466	1.02	P02461
Collagen I, α1	13	1464	0.89	P02452